CDDpress

www.nature.com/cdd

ARTICLE

Check for updates

Deubiquitinase OTUD6A in macrophages promotes intestinal inflammation and colitis via deubiquitination of NLRP3

Xin Liu[1,2], Yi Fang[1], Xinting Lv[2], Chenghong Hu[1], Guorong Chen[3], Lingxi Zhang[1], Bo Jin[1], Lijiang Huang[4], Wu Luo[1], Guang Liang[2] and Yi Wang[1,4,5]✉

Inflammatory bowel disease (IBD) is a chronic inflammatory disorder of the gastrointestinal tract, which has been shown to increase the incidence of colorectal cancer. Recent studies have highlighted the role of ubiquitination, a post-translational modification, in the occurrence and development of colonic inflammation. Ovarian tumor deubiquitinase 6 A (OTUD6A) is a deubiquitinating enzyme, which regulates cell proliferation and tumorigenesis. In this study, we investigated the expression and role of OTUD6A in IBD. Wide-type or *Otud6a*$^{-/-}$ mice were used to develop dextran sodium sulfate (DSS)- or 2,6,4-trinitrobenzene sulfonic acid (TNBS)-induced colitis model, as well as azoxymethane (AOM)/DSS-induced colitis-associated cancer model. Bone marrow-derived macrophages (BMDMs) were isolated from wild-type and *Otud6a*$^{-/-}$ mice to dissect molecular mechanisms. Our data show that OTUD6A deficiency attenuated DSS or TNBS-induced colitis, as well as AOM/DSS-induced colitis-related colon cancer in vivo. Bone marrow transplantation experiments further revealed that OTUD6A in myeloid cells was responsible for exacerbation of DSS-induced colitis. Mechanistically, OTUD6A directly bound to NACHT domain of NLRP3 inflammasome and selectively cleaved K48-linked polyubiquitin chains from NLRP3 at K430 and K689 to enhance the stability of NLRP3, leading to increased IL-1β level and inflammation. Taken together, our research identifies a new function of OTUD6A in the pathogenesis of colitis by promoting NLRP3 inflammasome activation, suggesting that OTUD6A could be a potential target for the treatment of IBD.

Cell Death & Differentiation (2023) 30:1457–1471; https://doi.org/10.1038/s41418-023-01148-7

INTRODUCTION

Inflammatory bowel diseases (IBDs), including Crohn's disease (CD) and ulcerative colitis (UC), are a series of heterogeneous chronic and relapsing inflammatory disorders of the digestive system, which are mainly driven by inappropriate mucosal immune responses to normal intestinal constituents. Recent studies reveal that innate immune cells, such as macrophages and neutrophils, infiltrate to the intestine during IBD with subsequent secretion of inflammatory cytokines [1, 2], leading to intestinal epithelial cells erosion and impairment of intestinal homeostasis [3, 4]. Moreover, IBD patients are known to be at higher risk for developing colitis-related colorectal cancer (CRC) [5, 6]. The colonic chronic inflammation initiates and promotes tumorigenesis, making IBD as one of the top three high-risk conditions for CRC [7]. Therefore, elucidating regulatory mechanisms of IBD and developing novel therapeutic targets based on IBD pathogenesis carry significant clinical values.

Although the progression of IBD is widely accepted to associate with multiple factors [8], ubiquitination, a post-translational modification, has been recently shown to regulate intestinal homeostasis and dysfunction [9]. Ubiquitination is a widespread protein modification that existed in many cellular processes in distinct manners [10]. It commonly occurs at lysine residues of substrate proteins, and the lysine residues of ubiquitin conclude Lys6, Lys11, Lys27, Lys29, Lys33, Lys48 and Lys63 [11]. The substrate specificity of ubiquitination mainly depends on E3 ubiquitin ligases. E3-mediated ubiquitination and deubiquitinases (DUBs)-mediated deubiquitination are two reversible processes that can target proteins involved in colonic inflammatory signaling pathways [12]. For example, deficiency of a deubiquitinase, USP47, resulted in the activation of NF-κB signaling pathway by increasing the K63-linked polyubiquitination of TRAF6 in intestinal epithelial cells [13]. Another deubiquitinase, ovarian tumor deubiquitinase 1 (OTUD1), exhibits an inhibitory effect on RIPK1-mediated NF-κB activation to prevent intestinal inflammation by specifically reversing K63-linked ubiquitination of RIPK1 [14]. Therefore, DUBs are critical for the intestinal immunomodulatory functions of immune cells. Ovarian tumor deubiquitinase 6 A (OTUD6A) is a recently identified deubiquitinase. Currently, only a few studies have been reported the role of OTUD6A in different cancers [15–17]. Although OTUD6A has been found aberrantly upregulated in colorectal cancer tissues [15], the potential role of OTUD6A in intestinal homeostasis, colitis, and colon cancer has not yet been elucidated.

In this study, the role of OTUD6A was examined in different models of colitis. We demonstrate that OTUD6A promotes intestinal

[1]Chemical Biology Research Center, School of Pharmaceutical Sciences, Wenzhou Medical University, Wenzhou, Zhejiang, China. [2]Affiliated Yongkang First People's Hospital and School of Pharmacy, Hangzhou Medical College, Hangzhou, Zhejiang, China. [3]Department of Pathology, the Affiliated Quzhou Hospital of Wenzhou Medical University, Quzhou, Zhejiang, China. [4]Department of Gastroenterology, the Affiliated Xiangshan Hospital of Wenzhou Medical University, Ningbo, Zhejiang, China. [5]School of Pharmacy, Hangzhou Normal University, Hangzhou, Zhejiang, China. ✉email: yi.wang1122@wmu.edu.cn

Received: 2 November 2022 Revised: 1 March 2023 Accepted: 7 March 2023
Published online: 17 March 2023

inflammation via impairing intestinal epithelium and promoting proinflammatory cytokine production. Furthermore, we confirm that OTUD6A in myeloid cells is responsible for the exacerbation of dextran sodium sulfate (DSS)-induced colitis. In addition, we show that OTUD6A specifically reverses K48-linked ubiquitination of NOD-like receptor family protein 3 (NLRP3) at K430 and K689, leading to stability and activation of NLRP3 inflammasome and induction of colonic inflammation in macrophages.

RESULTS

OTUD6A expression is upregulated in both UC patients and mice with colitis

To investigate the role of OTUD6A in IBD, we first analyzed the expression of OTUD6A in colon samples from UC patients and normal adjacent colon tissues obtained from colon cancer patients. We found that the expression of OTUD6A were significantly increased in patients with UC than those without UC (Supplementary Fig. S1A, B). We also found that the transcription of *Otud6a* in inflamed colon tissues from UC patients was higher than that in uninflamed colon tissues using an open-accessed Gene Expression Omnibus database (GSE11223) (Supplementary Fig. S1C). Furthermore, we found higher expression levels of OTUD6A in colon tissues from mice with colitis when compared to those from the healthy controls (Supplementary Fig. S1D, E). Collectively, these results suggest that increased OTUD6A expression was correlated with local colonic injuries in both humans and mice.

OTUD6A deficiency attenuates colitis-induced colonic injury

To identify the role of OTUD6A in colitis, age- and sex-matched wild-type (WT) and *Otud6a*$^{-/-}$ mice were used to develop DSS-induced acute colitis. As shown in Fig. 1A, the survival rate of *Otud6a*$^{-/-}$ mice was significantly higher than those of WT littermates after 3.5% DSS challenge ($P < 0.05$). Next, we treated *Otud6a*$^{-/-}$ and WT mice with 2.5% DSS to confirm the protective role of OTUD6A. Compared to the WT mice, *Otud6a*$^{-/-}$ mice showed reduced body weight loss (Fig. 1B) and displayed significantly longer colon tissues (Fig. 1C, D). Correspondingly, *Otud6a*$^{-/-}$ mice exhibited less colitis symptoms, including reduced stool consistency and rectal bleeding, which resulted in a lower disease activity index (DAI) as compared to the WT mice (Fig. 1E). Further histopathological examination revealed that the *Otud6a*$^{-/-}$ mice showed less disrupted colon epithelial barrier and less ulcerations than WT mice upon DSS challenge (Fig. 1F, G). PAS/AB staining also indicated that *Otud6a*$^{-/-}$ mice maintained more goblet cells than those of the WT mice after DSS treatment (Fig. 1H and Supplementary Fig. S2A). Ki67 staining showed that OTUD6A deletion reduced DSS-induced cell proliferation in colon tissues (Fig. 1I and Supplementary Fig. S2B). We also used 2,6,4-trinitrobenzene sulfonic acid (TNBS) to induce colitis in both WT and *Otud6a*$^{-/-}$ mice. Similarly, TNBS-induced colon shortening, body weight loss and epithelial damage were also alleviated in *Otud6a*$^{-/-}$ mice compared to the WT mice (Supplementary Fig. S3). These data indicate that OTUD6A deficiency significantly protected colon against DSS- or TNBS-induced injuries in mice.

OTUD6A deficiency decreases the production of proinflammatory cytokines

It is well accepted that proinflammatory cytokines are involved in intestinal inflammation [18]. To determine whether OTUD6A regulates inflammation in DSS-induced colitis, we first assessed the inflammatory infiltration and cell apoptosis in the colon tissues. Our data show that expression of F4/80 and LY6G was significantly reduced in colons of *Otud6a*$^{-/-}$ mice compared to those in the WT counterparts after DSS treatment, indicating that OTUD6A reduced DSS-induced infiltration of immune cells in colons (Fig. 2A and Supplementary Fig. S4A, B). In addition, TUNEL staining also indicated that *Otud6a*$^{-/-}$ mice showed less apoptosis cells in colon tissues when compared to those of the WT mice upon DSS challenge (Fig. 2A and Supplementary Fig. S4C). Consistent with these observations, the mRNA levels of proinflammatory cytokines and chemokines were significantly lower in the colons of *Otud6a*$^{-/-}$ mice than in those of WT mice (Fig. 2B). Next, we examined the protein level of IL-1β, which is a representative inflammatory cytokine in colitis. The data show that DSS challenge significantly increased IL-1β levels in both serum and colon tissues, while these changes were significantly reversed in *Otud6a*$^{-/-}$ mice in comparison to their WT littermates (Fig. 2C). Studies have demonstrated the importance of the NLRP3 inflammasome in IBD through upregulating IL-1β level [19, 20]. Thus, we examined the profile of NLRP3 in mouse colon tissues. Our Western blot data indicate that NLRP3 was dramatically increased in DSS-challenged WT mice, which was significantly reduced in *Otud6a*$^{-/-}$ littermates, indicating that NLRP3 may mediate the inflammatory regulation of OTUD6A (Fig. 2D, E). We also found that OTUD6A deficiency exhibited no significant effect on the expression of AIM2 and NLRC4 between DSS-treated WT and *Otud6a*$^{-/-}$ mice, suggesting that OTUD6A may specifically regulate NLRP3 inflammasome (Supplementary Fig. S5). Collectively, these results suggest that OTUD6A deficiency reduces NLRP3-mediated DSS-induced inflammatory responses in vivo.

OTUD6A expressed in myeloid cells is responsible for exacerbation of DSS-induced colitis

OTUD6A regulating NLRP3-driven inflammation promotes us to hypothesize that OTUD6A in macrophages may mainly contribute to inflammatory colitis. To confirm the role of OTUD6A in macrophages, bone marrow transplantation was employed using WT and *Otud6a*$^{-/-}$ mice to obtain myeloid cell-specific *Otud6a*$^{-/-}$ mice. Validation of bone marrow transplantation in chimeric mice was shown in Supplementary Fig. S6. We found that irradiated WT mice receiving *Otud6a*$^{-/-}$ bone marrow cells (KO → WT) were more resistant to DSS-induced colitis when compared to the irradiated WT mice receiving WT bone marrow cells (WT → WT), as evidenced by less weight loss and longer colon length (Fig. 3A–C). H&E and PAS/AB staining also showed reduced epithelial cell damage, less inflammatory cell infiltration and more goblet cells in the villi of the myeloid cell-specific *Otud6a*$^{-/-}$mice. Also, lower histology scores were found in the KO → WT group when compared to the WT → WT mice after DSS treatment (Fig. 3D–F). In addition, F4/80 and Ki67 positive cells were significantly decreased in KO → WT mice compared to the WT → WT mice after DSS challenge (Fig. 3G–I). Furthermore, the protein levels of IL-1β in both serum and colon tissues from KO → WT mice were significantly reduced when compared to those from the WT → WT mice (Fig. 3J, K). Interestingly, our data show that the protein levels of NLRP3 were markedly decreased in colon tissues in KO → WT mice compared to WT → WT mice after DSS induction (Fig. 3L). These results indicate that myeloid cell-specific OTUD6A knockout alleviates colitis and OTUD6A in macrophages is mainly responsible for exacerbation of DSS-induced colitis.

OTUD6A deficiency suppresses the development of AOM/DSS-induced colitis-associated colorectal cancer

IBD has been shown to increase the incidence of colorectal cancer [5, 6]. We further evaluated the role of OTUD6A in the development of colitis-associated colorectal cancer using a well-recognized AOM/DSS-induced mouse model. The schematic timeline of the animal experiment is shown in Fig. 4A. The results showed that the *Otud6a*$^{-/-}$ mice exhibited less body weight loss and had a higher survival rate as compared to WT mice after AOM/DSS treatment (Fig. 4B, C). In addition, AOM/DSS-treated *Otud6a*$^{-/-}$mice developed less and smaller colon tumors compared with the WT littermates (Fig. 4D–F). H&E staining also showed low-grade dysplasia in the colons of the *Otud6a*$^{-/-}$ mice, while high-grade dysplasia of

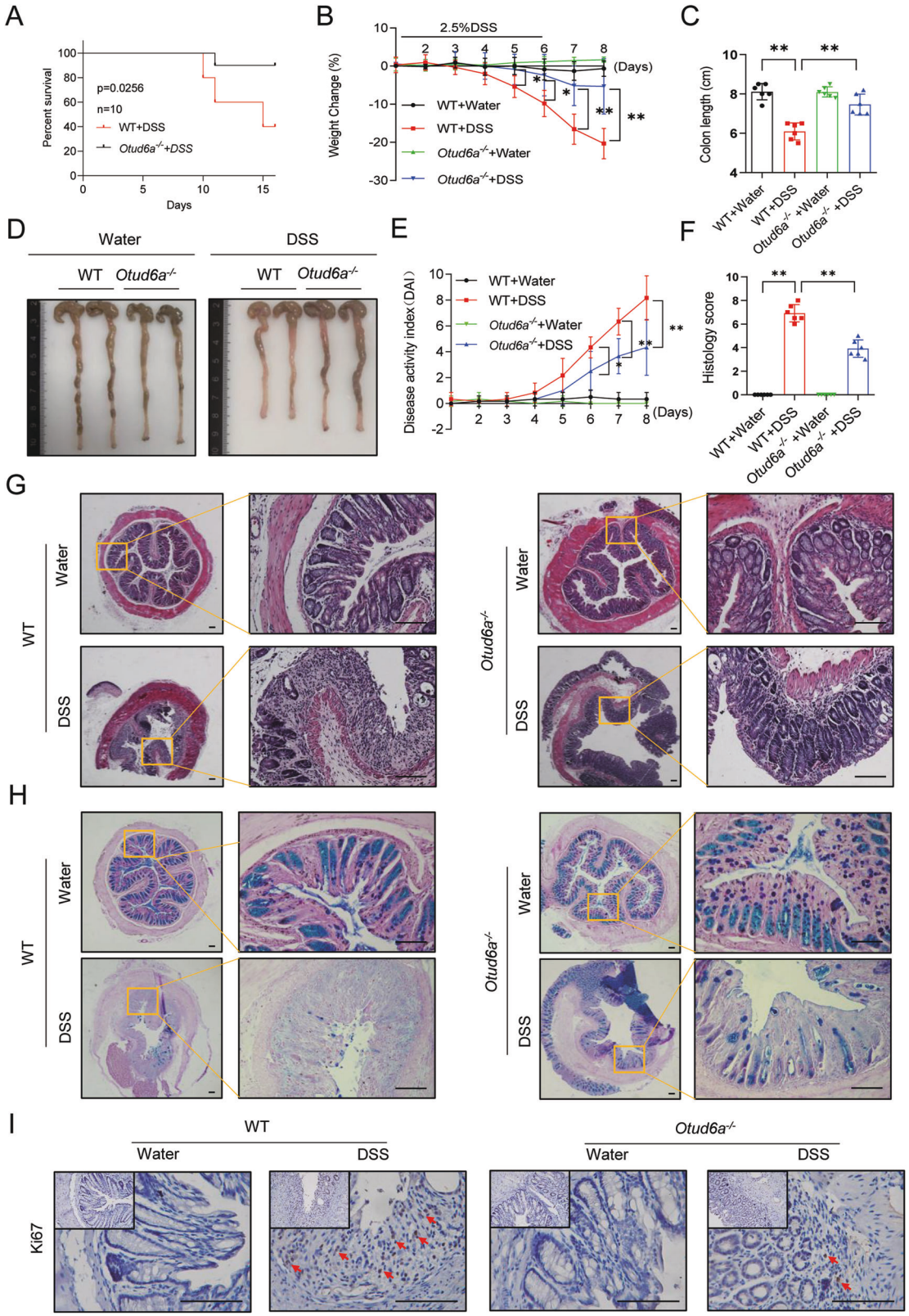

Fig. 1 OTUD6A deficiency attenuated colonic injury induced by colitis. A Survival (Kaplan-Meier) curves ($n = 10$) of WT and *Otud6a*$^{-/-}$ mice with 3.5% DSS-induced colitis. **B** Body weight change ($n = 6$) of WT and *Otud6a*$^{-/-}$ mice with 2.5% DSS-induced colitis. Colon length (**C**) and representative images of colon tissues (**D**) from the indicated treatment groups at day 8 after DSS treatment ($n = 6$). Disease activity index (**E**) and semi-quantitative scoring of histopathology on day 8 after DSS administration (**F**) were shown ($n = 6$). Representative images of H&E (**G**), PAS staining (**H**) and Ki67 staining (**I**) in cross-sections of distal colon tissues from WT and *Otud6a*$^{-/-}$ mice on day 8 after DSS administration. Scale bars = 100 μm. Statistical data are presented as mean ± SD. *$P < 0.05$, **$P < 0.01$.

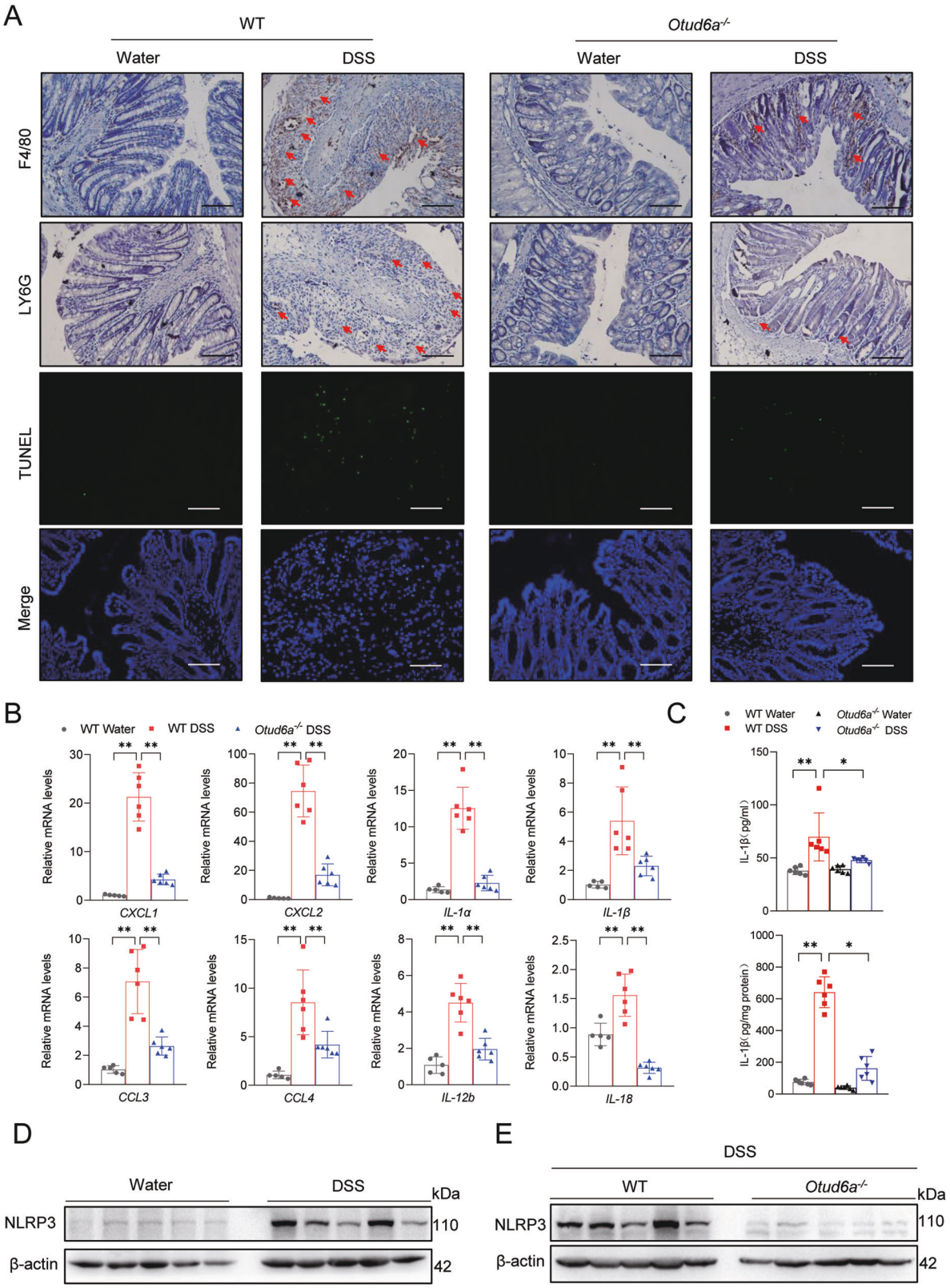

Fig. 2 OTUD6A deficiency decreases the inflammatory infiltration and production of proinflammatory cytokines. A Representative images of F4/80, LY6G and TUNEL staining in cross-sections of distal colon from WT and *Otud6a*$^{-/-}$ mice on day 8 after DSS administration. Scale bar = 100 μm. **B** mRNA levels of the proinflammatory genes in colon sections from WT and *Otud6a*$^{-/-}$ mice after DSS treatment ($n = 6$). **C** IL-1β levels in serum (upper panel) and colon tissues (lower panel) from WT and *Otud6a*$^{-/-}$ mice treated with 2.5% DSS were measured via ELISA ($n = 6$). **D**, **E** Immunoblot analysis of NLRP3 in the distal colons of the control and DSS-treated mice. β-actin was used as the loading control ($n = 5$). Data are presented as mean ± SD. *$P < 0.05$, **$P < 0.01$, and ***$P < 0.001$.

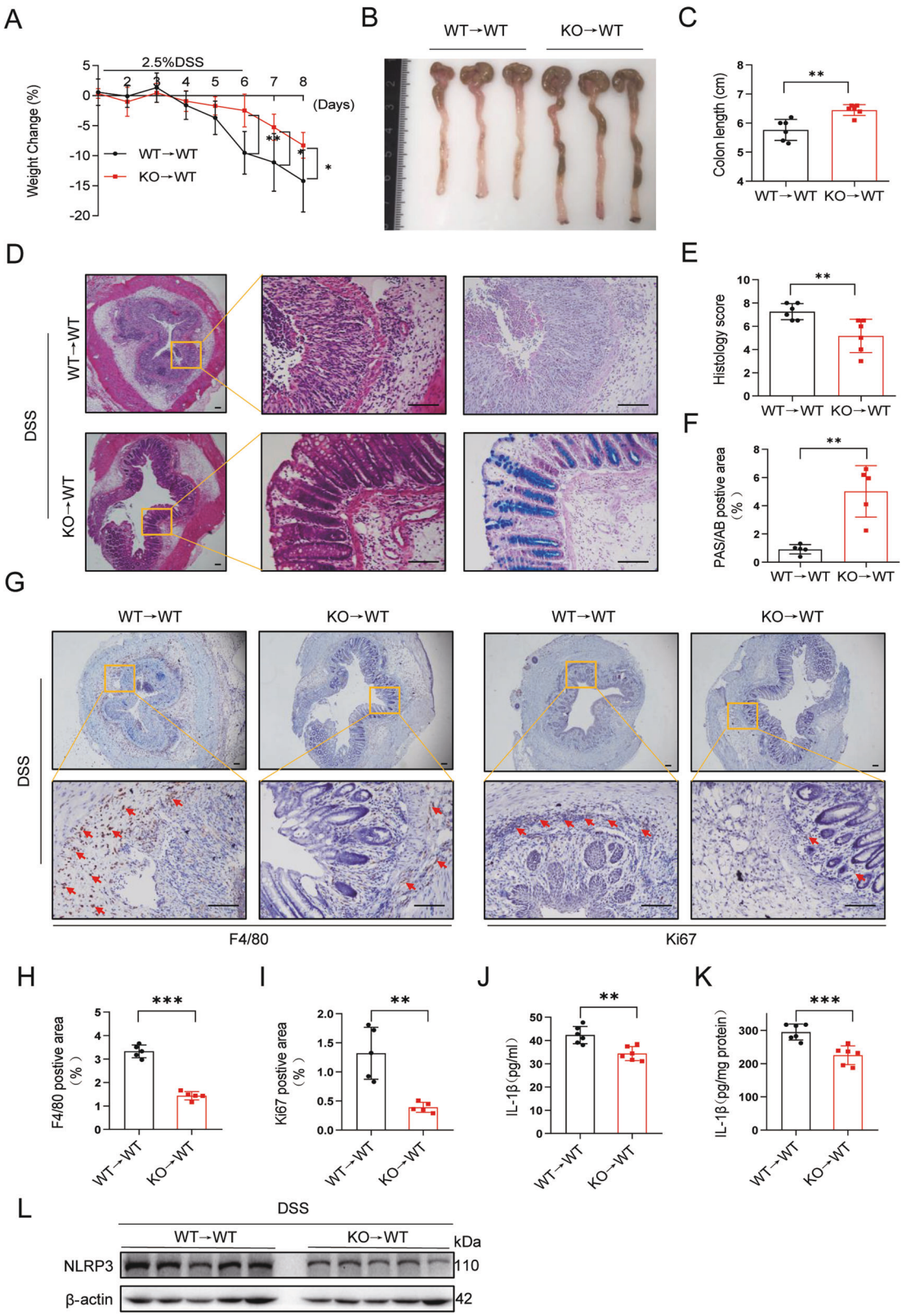

adenomas in the WT littermates (Fig. 4G left panel). Immunohistochemical staining data also revealed a significant decrease of Ki67-positive (Fig. 4G middle panel) and NLRP3-positive cells (Fig. 4G right panel) in the colon tissues from *Otud6a*$^{-/-}$ mice compared to those of the WT mice upon AOM/DSS challenge. Moreover, protein levels of IL-1β in the serum or colon tissues of *Otud6a*$^{-/-}$ mice were significantly reduced compared with those of the WT littermates (Fig. 4H). In addition, immunoblot and immunofluorescence analyses revealed that NLRP3 expression was markedly reduced in the colon tumors of AOM/DSS-treated *Otud6a*$^{-/-}$ mice (Fig. 4I and Supplementary Fig. S7). Collectively, these data confirm that OTUD6A suppresses the development of AOM/DSS-induced

Fig. 3 Deficiency of OTUD6A in myeloid cells alleviates DSS-induced colitis. A Two groups of chimeric mice (WT → WT and KO → WT) generated by bone marrow transplantations were exposed to 2.5% DSS for 6 days and followed by 2 days regular drinking water, and body weight changes were daily monitored ($n = 6$). **B**, **C** Representative images of colons and colon length from the two groups at day 8 after DSS treatment ($n = 6$). Representative images of H&E and PAS/AB staining in distal colon cross-sections (**D**) and semi-quantitative scoring of histopathology (**E**) and quantification of PAS/AB staining area (**F**) ($n = 5$-6), scale bars = 100 μm. **G** Representative images of F4/80 and Ki67 staining in distal colon cross-sections of chimeric mice described in **B**. Quantification of F4/80 staining area (**H**), and Ki67 staining area (**I**). ELISA evaluation of IL-1β levels in serum (**J**) and colon tissues (**K**) from WT → WT and KO → WT mice treated with 2.5% DSS ($n = 6$). **L** Immunoblot analysis of the NLRP3 levels in the distal colons of DSS-treated mice. β-actin was used as the loading control ($n = 5$). Data are presented as mean ± SD. $^{**}P < 0.01$, and $^{***}P < 0.001$.

colitis-associated colorectal cancer, accompanied with decreased NLRP3/IL-1β levels in colon tissues.

OTUD6A promotes NLRP3 inflammasome activation in macrophages

Next, we investigated the effect of OTUD6A on NLRP3 inflammasome activation in macrophages. Primary BMDMs from WT and *Otud6a*$^{-/-}$ mice were used to evaluate the secretion of IL-1β primed by different stimulators. As shown in Fig. 5A, the expression of IL-1β was markedly reduced in *Otud6a*$^{-/-}$ BMDMs treated with LPS + ATP and nigerian but not poly(dA:dT) transfection as compared to the WT BMDMs. Similar to the in vivo study, OTUD6A deficiency did not affect the expression of AIM2 and NLRC4 in LPS-treated BMDMs (Supplementary Fig. S8). Also, OTUD6A deficiency exhibited no inhibitory effect on the secretion of TNF-α, indicating that OTUD6A did not affect the NF-κB-mediated inflammatory pathway (Fig. 5B). Next, the role of OTUD6A in regulating NLRP3 inflammasome activation was further confirmed by immunoblotting. Our data show that OTUD6A deficiency reduced the secretion of mature IL-1β p17 and cleaved caspase-1 p20 in macrophages upon stimulation by LPS and ATP (Fig. 5C). We then evaluated the release of LDH to see the subsequent cell death and found that decreased LDH release in *Otud6a*$^{-/-}$ macrophages after ATP or nigerian treatment (Fig. 5D). In addition, our data show that ASC specks formation in LPS-primed and nigerian-challenged macrophages was significantly reduced in *Otud6a*$^{-/-}$ BMDMs when compared to the WT BMDMs, indicating decreased NLRP3 activity in *Otud6a*$^{-/-}$ BMDMs (Fig. 5E, F). To further examine whether the activation of NLRP3 inflammasome is affected by OTUD6A, we overexpressed OTUD6A through transfecting the OTUD6A plasmid to BMDMs from WT and *Nlrp3*$^{-/-}$ mice, then stimulated the macrophages with LPS and ATP. As shown in Fig. 5G, H, flag-labeled OTUD6A plasmid transfection increased NLRP3 level and IL-1β production in BMDMs challenged by LPS + ATP, while NLRP3 knockout almost completely inhibited the secretion of IL-1β in OTUD6A-overexpressed BMDMs. These results suggest that the activation of NLRP3 is regulated by OTUD6A.

OTUD6A directly interacts with NLRP3

Studies have shown that the ubiquitinating/deubiquitinating regulation of NLRP3 is important for the stability and activation of NLRP3 inflammasome [21–24]. To determine whether OTUD6A deubiquitinates NLRP3, we first determined whether OTUD6A is able to physically associate with NLRP3. Co-immunoprecipitation (Co-IP) experiments and double immunofluorescence staining demonstrated a direct interaction between OTUD6A and NLRP3 (Fig. 6A, B). Immunoprecipitation analysis further confirmed the interaction of OTUD6A with NLRP3 via in vitro co-transfection of OTUD6A-Flag and NLRP3-HA plasmids (Fig. 6C, D). To further explore which domain of OTUD6A is essential for the interaction with NLRP3, we constructed different OTUD6A-Flag truncations and co-transfected them into HEK293T cells with vector control and full-length NLRP3-HA plasmids as comparisons (Fig. 6E). Co-IP analysis revealed that the OTU domain (residues 141–275) of OTUD6A were indispensable for binding to NLRP3 (Fig. 6F). Later a series of Flag-tagged NLRP3 truncated mutants were also constructed to identify the key domain in NLRP3 protein (Fig. 6G). As shown in Fig. 6H, we found that the NACHT domain of NLRP3 mainly contributed to the interaction between NLRP3 and OTUD6A. Finally, the interaction between endogenous OTUD6A and NLRP3 in BMDMs was confirmed by Co-IP assay under physiological conditions. Figure 6I shows that the interaction between OTUD6A and NLRP3 was increased after LPS + ATP challenge. These data confirm the direct interaction between OTUD6A and NLRP3.

OTUD6A stabilizes NLRP3 via its deubiquitination activity

We next investigated the molecular mechanism by which OTUD6A regulates NLRP3 activity. Firstly, NLRP3-HA was co-transfected with Ub-Myc and OTUD6A-Flag into HEK293T cells. As shown in Fig. 7A, the ubiquitination of NLRP3 was markedly reduced in the presence of OTUD6A, and OTUD6A significantly increased the protein levels of NLRP3-HA through promoting its deubiquitination. Next, proteasome and autolysosome inhibitors were used to determine which pathway may affect the OTUD6A-mediated NLRP3 stability. Interestingly, proteasome inhibitor MG132, but not lysosome inhibitor chloroquine (CQ) or autophagy inhibitor 3-methyladenine (3-MA), abolished the NLRP3 protein expression (Supplementary Fig. S9). Cys152 in OTU domain has been reported as the key site for the deubiquitinating enzymatic activity of OTUD6A [15]. We constructed the a Cys152-mutant plasmid (OTUD6A-C152A-Flag) and transfected it into HEK293T cells, together with NLRP3-HA and Ub-Myc. The data show that OTUD6A mutation at C152A significantly decreased the ability of its deubiquitination and reduced the stability of NLRP3 (Fig. 7B). Moreover, OTUD6A increased the deubiquitination and stability of NLRP3 in a dose-dependent manner in HEK293T cells (Fig. 7C). Similarly, exogenously expressed OTUD6A increased the level of NLRP3 in HEK293 cells, while the catalytic-dead OTUD6A-C152A mutant did not (Fig. 7D). Furthermore, our data show that OTUD6A deficiency significantly increased endogenous NLRP3 ubiquitination in response to LPS + ATP stimulation under physiological condition (Fig. 7E). In addition, we performed a cycloheximide chase assay and demonstrated that OTUD6A deficiency markedly shorted the half-life of endogenous NLRP3 protein in BMDMs (Fig. 7F). Collectively, these data suggest that OTUD6A directly deubiquitinates NLRP3 to inhibit its proteasomal degradation and enhance its stability and level.

OTUD6A mediates K48-linked deubiquitination of NLRP3 at lysine 430 and lysine 689

NLRP3 has been reported to be modified by different forms of ubiquitination, including K27, K48 and K63 [25–27]. To further determine which type of ubiquitin chain on NLRP3 was affected by OTUD6, we then performed deubiquitination assays with a series of ubiquitin isoforms and mutants. Figure 8A shows that OTUD6A mainly removed K11-, K27-, K48- and K63-linked ubiquitin chains from NLRP3 and obviously enhanced the protein levels of NLRP3. Next, K11R, K27R, K48R and K63R mutants were used to repeat the deubiquitination assays. As shown in Fig. 8B and Supplementary Fig. S10A–C, only K48R mutation reversed the deubiquitination activity of OTUD6A on NLRP3, indicating that OTUD6A mainly mediates K48-linked deubiquitination of NLRP3, rather than K11R-, K27R- and K63R-linked deubiquitination. Furthermore, we identified which lysine residues in NLRP3 may be associated with this deubiquitination modification by OTUD6A. Thus, we substituted five key ubiquitination sites in NLRP3 with

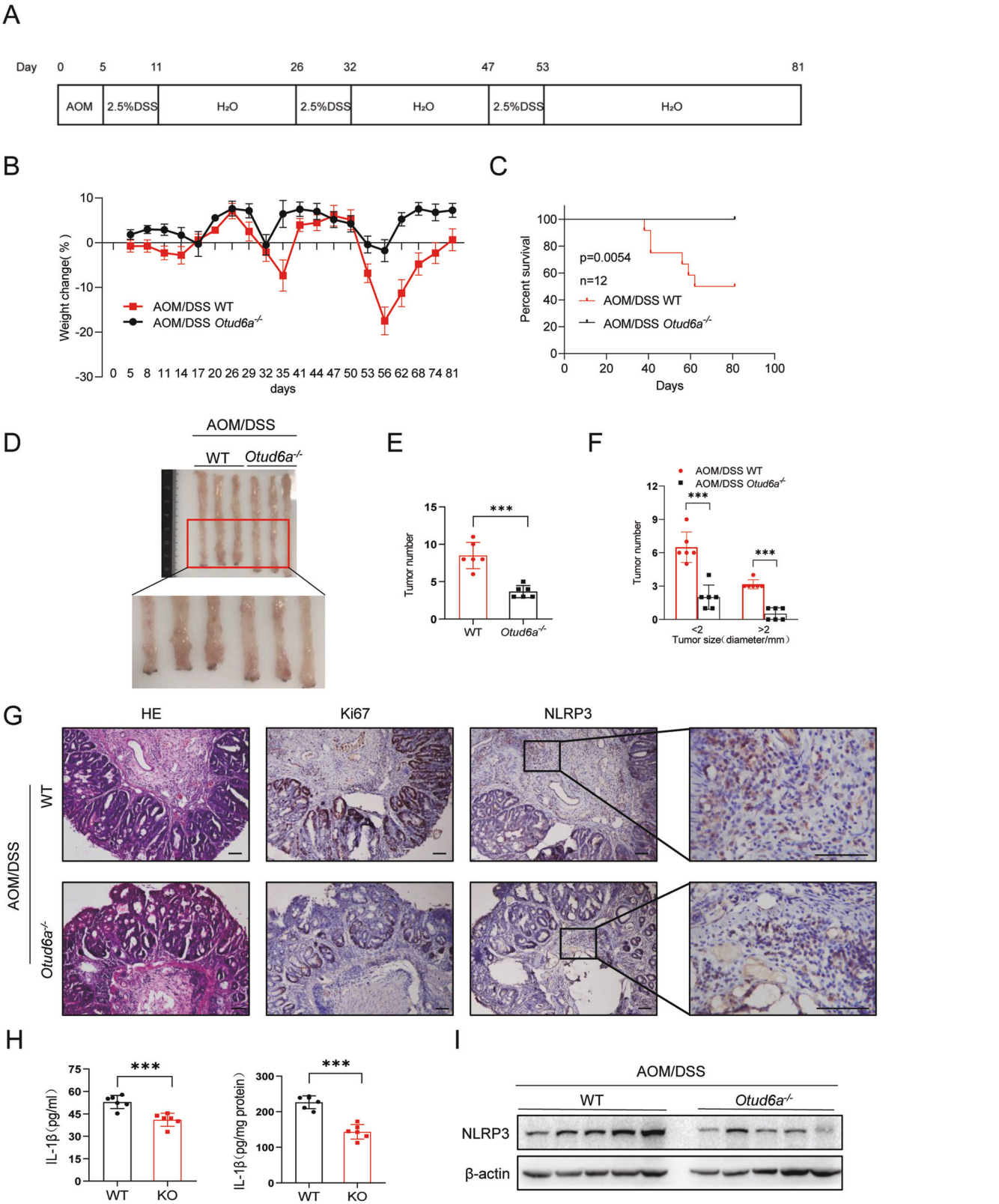

Arg to create the K324R, K357R, K430R, K496R and K689R NLRP3 mutants. As shown in Fig. 8C, overexpression of OTUD6A increased the protein levels of NLRP3 in HEK293 cells when co-transfected with K324R, K357R, and K496R mutants, but not in cells co-transfected with K430R or K689R mutants, suggesting that K430 and K689 in NLRP3 were required for OTUD6A-mediated NLRP3 accumulation. Further assays also confirmed that the deubiquitination of NLRP3 was reversed by OTUD6A when K430R and K689R mutants were transfected (Fig. 8D). Collectively, these findings demonstrate that OTUD6A cleaves the K48-linked polyubiquitin of NLRP3 at K430 and K689, leading to inhibition of the proteasomal degradation of NLRP3.

Fig. 4 OTUD6A deficiency suppresses AOM/DSS-induced colon cancer. A A schematic overview of the colitis associated cancer model. Sex- and age-matched WT and *Otud6a*$^{-/-}$ mice ($n = 6$) were used for the experiments. Five days after the initial AOM injection (10 mg/kg), 2.5% DSS was given in drinking water for 6 days followed by regular water for 15 days, and this cycle was repeated twice. **B** Body weight of AOM/DSS-treated mice during the experiment. **C** Sex- and age-matched WT and *Otud6a*$^{-/-}$ mice ($n = 12$) mice were used for the experiments. Five days after the initial AOM injection (10 mg/kg), 2.5% DSS was given in drinking water for 7 days followed by regular water for 14 days, and this cycle was repeated twice. The survival curve of WT and *Otud6a*$^{-/-}$ mice in AOM/DSS-treated animals. **D–F** After the procedures described in **A**, representative images of colons from WT and *Otud6a*$^{-/-}$ mice after AOM/DSS treatment (**D**). The tumor numbers (**E**) and tumor sizes (**F**) were measured. The results shown are the mean ± SD values; $n = 6$. **G** Representative images of H&E staining and immunohistochemical staining of colon tumors from WT and *Otud6a*$^{-/-}$ mice described in **D**. Scale bars = 100 μm. **H** ELISA measurement of the IL-1β levels in serum (left panel) and colon tissues (right panel) from WT and *Otud6a*$^{-/-}$ mice treated with AOM/DSS ($n = 6$). **I** Immunoblot analysis of the NLRP3 levels in the colon tumor tissues of AOM/DSS-treated mice. β-actin was used as the loading control ($n = 5$). Data are presented as the means ± SD. ***$P < 0.001$.

DISCUSSION

In this study, we demonstrate that a deubiquitinase, OTUD6A, enhances NLRP3 stability and then promotes NLRP3 inflammasome activation and IL-1β secretion in mouse macrophages, leading to the development of colitis. Our results also reveal a mechanism underlying OTUD6A-mediated activation of NLRP3 inflammasome: 1) OTUD6A directly binds to the NACHT domain of NLRP3; 2) OTUD6A cleaves the K48-linked polyubiquitin of NLRP3 at K430 and K689, leading to inhibition of the proteasomal degradation of NLRP3 to enhance NLRP3 stability and protein level. Phenotypically, knockout of OTUD6A significantly alleviates DSS/TNBS-induced inflammatory colitis and reduces the CRC development induced by AOM/DSS in mice. A schematic illustration of the main findings is shown in the Graphical Abstract. Our data support that targeting OTUD6A could be a potential therapeutic approach for IBD.

It is well accepted that aberrant and continuing inflammatory responses caused by foreign or domestic threats contribute to the pathogenesis of IBD. Several DUBs have been shown to contribute to the pathogenesis of IBD by altering intestinal barrier functions and immune responses [9]. Deficiency of A20, a DUB in the OTU family, in macrophages promotes pro-inflammatory cytokine expression in macrophages through the NF-κB signal pathway and aggravates the pathogenesis of DSS-induced colitis in mice [28]. A20 has also been shown to inhibit necroptosis of intestinal epithelial cells by removing K63-linked polyubiquitin chains from RIPK3 [29]. OTUD6A has been originally reported as an oncogene. For example, OTUD6A is shown to promote prostatic tumorigenesis through deubiquitinating and stabilizing c-Myc [16]. OTUD6A also promotes tumor cell resistance to chemoradiotherapy by deubiquitinating and stabilizing TopBP1 [17]. Previously, it has been observed that the expression of OTUD6A is upregulated in colon cancer tissues when compared to the normal colonic tissues [15]. Here, our results show increased expression of OTUD6A not only in the colons of mice after DSS administration, but also in the intestinal samples of UC patients. Moreover, *Otud6a*$^{-/-}$ mice were more resistant to DSS- and TNBS-induced colitis with less inflammatory cell infiltration into the colon tissues. Furthermore, bone marrow transplantation confirms that OTUD6A in myeloid cells were responsible for attenuation of DSS-induced colitis by reducing the expression of NLRP3 and the release of IL-1β. In addition, our study suggests that *Otud6a*$^{-/-}$ mice developed less, smaller, and lower-grade colon tumors compared with their WT littermates in the AOM/DSS model. These results suggest a novel function of OTUD6A in both colitis and CRC development.

As an important intracellular pattern-recognition receptor, NLRP3 has been shown to be widely involved in many inflammatory diseases [30–32]. Especially, several studies have revealed the essential role of NLRP3 in maintaining intestinal epithelial homeostasis [26, 33]. For example, overactivation of NLRP3 inflammasome and increased proinflammatory cytokines are major clinical manifestations of most IBD patients in clinic [34]. In addition, *Nlrp3*$^{-/-}$ mice show less colonic tissue lesions and lower levels of proinflammatory cytokines released than the WT mice [35]. Considering the colitis-promoting role of NLRP3, targeting NLRP3 could be an attractive therapeutic strategy for IBD. However, only a few NLRP3 inhibitors are available in preclinical studies now, including MCC950, IFM-2427, Inzomelid and Somalix [36]. Unfortunately, due to the structural complexity of the NLRP3 inflammasome and off-target effects of the small-molecule NLRP3 inhibitors, none of the current NLRP3 inhibitors has been approved by FDA so far. For instance, as one of the first discovered specific small-molecule NLRP3 inhibitors, MCC950 shows promising therapeutic effects in the treatment of many inflammatory diseases in preclinical studies [36]. However, clinical trials of MCC950 showed increased serum liver enzyme levels, indicating its potential hepatotoxicity [36]. Thus, identifying novel strategies (e.g. ubiquitinating/deubiquitinating modification) to endogenously modulate the level and activity of NLRP3 may benefit the treatment of IBD.

The activation of NLRP3 inflammasome is tightly regulated by different regulatory factors in macrophages. The deubiquitination of NLRP3, which is an early priming event, is considered to be an important regulation for NLRP3 inflammasome activation [37]. Usually, NLRP3 remains inactive via ubiquitination under resting conditions. Under challenge of stimuli, NLRP3 is deubiquitinated and activated, leading to maturation and secretion of IL-1β and IL-18, followed by the induction of pyroptosis [38]. NLRP3 has been reported to be involved in various types of ubiquitination or deubiquitination modifications [25, 26, 39, 40]. Previous studies have revealed that TRIM31, an E3 ligase constitutively expressed in the gut, attenuates NLRP3 inflammasome activation by promoting proteasomal degradation of NLRP3 via K48-linked polyubiquitination [26]. USP19 specifically cleaved the K6-linked polyubiquitin chain of NLRP3 at K689 and inhibits the proteasomal degradation of NLRP3 [24]. RNF125 and Cbl-b as the key E3 ubiquitin ligases keep NLRP3 inflammasomes in check by targeting NLRP3 for sequential K63- and K48-linked polyubiquitination [41]. It is also report that YAP promotes the activation of NLRP3 inflammasome via blocking K27-linked polyubiquitination of NLRP3 [25]. Here, we identified OTUD6A as a novel DUB targeting NLRP3. OTUD6A mainly removes K48-linked ubiquitination of NLRP3 at K430 and K689 and inhibits the proteasomal degradation of NLRP3. Moreover, we confirmed that the NACHT domain of NLRP3 mainly contributed to the interaction with OTUD6A. Generally, the NACHT domain is responsible for the self-oligomerization of NLRP3 during the activation of NLRP3 inflammasome. Future structural biology investigations are needed to further clarify the specific binding site and deubiquitinating mode between OTUD6A and NLRP3.

As seen in our data, OTUD6A deficiency only partially reduced the protein level of pro-IL-1β and NLRP3 in *Otud6a*$^{-/-}$ BMDMs, it might raise the possibility of hypo-priming in *Otud6a*$^{-/-}$ BMDMs. For this concern, we performed RNA-sequencing analysis using LPS-stimulated WT and *Otud6a*$^{-/-}$ BMDMs. Our data show that OTUD6A deficiency do not affect LPS-induced gene expression of *Nfkb*, *Tnfa* and *Nlrp3* (Supplementary Fig. S11A–C). Our RT-qPCR and ELISA analysis further confirmed this result in BMDMs or mouse colon tissues (Supplementary Fig. S11D–F). These data conclude that OTUD6A deficiency did not affect NF-κB activation and NLRP3 priming in *Otud6a*$^{-/-}$ BMDMs. Finally, the impact

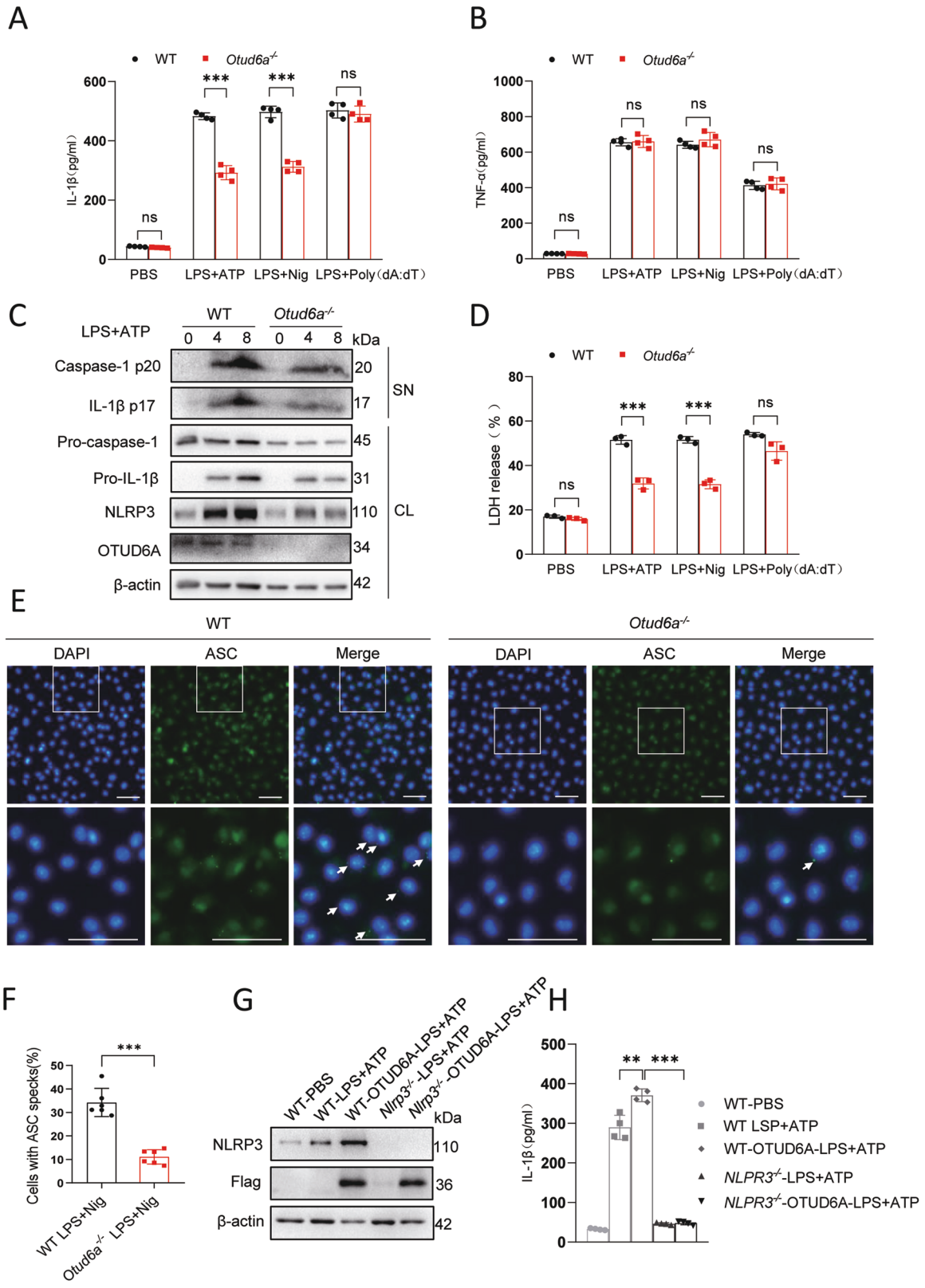

of OTUD6A deficiency on LPS-induced septic mouse model was also evaluated. As shown in Supplementary Fig. S12, IL-1β secretion in the serum was significantly reduced in *Otud6a*$^{-/-}$ mice while the TNF-α production were not affected. These data suggest that similar role of OTUD6A might be also found in other NLRP3-driven diseases. However, further studies are need to confirm this hypothesis.

In summary, our findings prove that OTUD6A promotes NLRP3 stability and increases NLRP3 level in macrophages through K48-linked deubiquitination, which promotes colon

Fig. 5 Inhibition of OTUD6A blocks the activation of NLRP3 inflammasome. A, **B** BMDMs from WT and *Otud6a*$^{-/-}$ mice were primed with LPS (100 ng/ml) for 4 h, followed by treatment of ATP (2 mM) or nigericin (10 μM) for 30 min or poly(dA:dT) transfection for 3 h. IL-1β and TNF-α released in the supernatant was measured by ELISA analysis ($n = 4$). **C** Immunoblot analysis of indicated proteins in supernatants (SN) or cell lysates (CL) of BMDMs from WT or *Otud6a*$^{-/-}$ mice, primed with LPS, and followed by ATP for 30 min. **D** LDH release from supernatant of BMDMs from WT and *Otud6a*$^{-/-}$ mice primed with LPS (100 ng/ml) for 4 h and treated with ATP (2 mM) or nigericin (10 μM) for 30 min or poly(dA:dT) transfection for 3 h, ($n = 3$). **E** Arrows showing ASC specks immunofluorescence in BMDMs from WT and *Otud6a*$^{-/-}$ mice primed with LPS (100 ng/ml) for 4 h followed by treatment with 10 μM nigericin for 45 min. scale bar = 100 μm. **F** Quantification of ASC speck formations. **G** Representative immunoblot analysis of NLRP3 expression in the cell lysates as describes in **C**. β-actin was used as the loading control. **H** ELISA evaluation of IL-1β levels in supernatants of BMDMs from WT or *Nlrp3*$^{-/-}$ mice transfected with control or OTUD6A plasmid, primed with LPS for 8 h, and followed by stimulation with ATP for 30 min. Data are presented as mean ± SD. $^{**}P < 0.01$, and $^{***}P < 0.001$.

inflammation and facilitates the pathogenesis of DSS-induced colitis. These studies have discovered macrophage OTUD6A as an important factor in IBD through directly regulating NLRP3 stability and provide that OTUD6A blockade might be a potential therapeutic approach for chronic intestinal inflammatory diseases such as IBD and CRC.

MATERIALS AND METHODS

Cell culture and reagents

HEK293T cells (Cat#: GNHu17) and L-929 cells (Cat#: GNM28) were purchased from National Collection of Authenticated Cell Cultures (Shanghai, China). 293 T cells were cultured in DMEM (Gibco) with 10% fetal bovine serum (FBS; Gibco, Eggenstein, Germany). L929 cells were cultured in MEM-α (Gibco) medium supplemented with 10% FBS. LPS (Cat#: L2880), ATP (Cat#: A3377), cycloheximide (Cat#: C4859), azoxymethane (Cat#: A5486), 2,6,4-trinitrobenzene sulfonic acid (TNBS, Cat#: P2297) were from Sigma-Aldrich (St Louis, MO). MG132 (Cat#: T2154), 3-Methyladenine (Cat#: T1879), Chloroquine (Cat#: T8689) were from TargetMol (shanghai, China). Poly(dA:dT) (cat#:tlrl-patn) was from InvivoGen (San Diego, CA, USA). Dextran sulfate sodium (DSS, Cat#: 0216011080, 36–50 kDa) was bought from MP Biomeicals (Aurora, OH). Anti-Asc (Cat#:AG-25B-0006), anti-NLRP3 (Cat#: AG-20B-0014) and anti-caspase-1 p45&p20 (Cat#: AG-20B-0042) were from AdipoGen (San Diego, CA); anti-MYC-Tag (Cat#: 2276), anti-F4/80 (Cat#: 70076), anti-Ki67 (Cat#: 9449) and HRP-linked second Antibody (Cat#: 7074, Cat#: 7076, Cat#: 7077) were from Cell Signaling Technology (Beverly, MA); anti-OTUD6A, anti-HA-Tag (Cat#: 51064-2-AP), anti-Flag-Tag (Cat#: 66008-4-Ig), anti-β-actin (Cat#: 66009-1-Ig) were from Proteinthch (Wuhan, China); Anti-NLRC4 (ab201792), anti-DUBA2(ab185352) and anti-Ly6g + Ly6c (Cat#: ab25377) were from Abcam (Cambridge, MA); Anti-AIM2 (sc-515642) and anti-ubiquitin (sc-8017) were from Santa Cruz, CA. Nigericin (cat#:HY-100381) and anti-HA Magnetic Beads (Cat#: HY-K0201) were from MCE (Shanghai, China). Protein A + G Agarose (Cat#: P2055) used for immunoprecipitation was from Beyotime (Shanghai, China). MonoRab™ Anti-Flag Magnetic Beads (Cat#: L00835) was from GenScript (Nanjing, China).

Plasmids construction and transfection

NLRP3-Flag plasmid was purchased from Genechem (Shanghai, China). OTUD6A-flag, OTUD6A-C152A-Flag, GFP-△OTU-Flag, GFP-△NT-Flag, △CT-Flag and OTUD6A-HA plasmids were purchased from Tsingke Biotechnology (Beijing, China). NLRP3-HA, PYD-Flag, NACHT-Flag and LRR-Flag plasmids were purchased from GENEWIZ (Suzhou, China). Expression vectors for Myc-Ub WT, Myc-Ub-K6, Myc-Ub-K11, Myc-Ub-K27, Myc-Ub-K29, Myc-Ub-K33, Myc-Ub-K48, Myc-Ub-K63, Myc-Ub-K11R, Myc-Ub-K27R, Myc-Ub-K48R, Myc-Ub-K63R and Flag-NLRP3-K324R, Flag-NLRP3-K357R, Flag-NLRP3-K430R, Flag-NLRP3-K496R, Flag-NLRP3-K689R plasmids were purchased from keLei Biological Technology (Shanghai, China). All constructs were confirmed by DNA sequencing. Plasmids were transiently transfected into HEK293T cells with lipofectamine3000 reagent (Invitrogen, Carlsbad, CA) according to the manufacturer's instructions.

Human samples

A total of 10 colonic biopsy samples were collected from patients with UC who were hospitalized in Quzhou People's Hospital. Another 10 colon samples were obtained from normal adjacent colon tissues of colon cancer patients admitted for colectomy surgery. The study was approved by the Human Ethical Committee of the Quzhou People's Hospital (Approval document #2022–0037). Basic information concerning the patients, including age and sex, is summarized in Supplementary Table S1.

Animals

C57BL/6 J mice were obtained from. OTUD6A knockout (C57BL/6 J background, *OTUD6A*$^{-/-}$) mice were from Professor Fuping You (Peking University, Beijing, China). NLRP3 knockout (C57BL/6 J background, *Nlrp3*$^{-/-}$) mice were purchased from VIEWSOLID (Beijing, China). All mice were housed under specific-pathogen free conditions with 50 ± 5% humidity at 22 ± 2 °C with a 12/12 h light/dark cycle. All animal studies were approved by the Institutional Animal Policy and Welfare Committee of Wenzhou Medical University (Approval document #wydw2022-0202).

DSS-induced colitis and colitis-associated colorectal cancer models

For the DSS-induced colitis model, 8-week-old male mice were administered with 2.5% DSS in drinking water for 6 days, followed by 2 days of regular drinking water. The mice were sacrificed on day 8 under anesthesia. For survival analysis experiments, 3.5% DSS in drinking water was administered for 6 days, followed by regular drinking water until day 16.

For TNBS-induced colitis model, co-housed experimental mice were injected with 2.5% TNBS that was dissolved in ethanol on day 1. The mice were sacrificed on day 5 under anesthesia.

For the AOM/DSS induced colitis-associated colorectal cancer model, co-housed experimental mice were treated with AOM at 10 mg/kg in PBS via intraperitoneal (i.p.) injection on Day 0. Five days later, DSS (2.5%) was given in drinking water for 6 days, followed by regular water for 15 days. After 3 cycles of DSS treatment, the mice were sacrificed on day 81 under anesthesia.

Isolation of bone marrow-derived macrophages

Bone marrow-derived macrophages (BMDMs) were isolated from the femur and tibia of mice as previously described [42]. Briefly, femur and tibia were flushed with RPMI 1640 containing penicillin (100 units/mL) and streptomycin (100 μg/mL). Then the samples were filtered using 70-mm nylon meshes. After centrifugation at 1100 *g* for 5 min, bone marrow cells were collected and cultured in DMEM containing 20% L-929 culture medium and 10% fetal bovine serum. On day 3 and day 5, fresh DMEM containing 20% L-929 culture medium and 10% fetal bovine serum was added. Cells were used for experiments on day 7.

Bone marrow chimeric mouse model

Bone marrow chimeric mice were established as previously described [42]. Recipient mice were subjected to irradiation with a dose of 6 Gy. The bone marrow cells were isolated from WT or *Otud6a*$^{-/-}$ (KO) mice, respectively. A total of 5.0×10^6 donor bone marrow cells were injected into each irradiated WT recipient mouse via tail vein (i.v.) injection. Eight weeks later, the WT → WT and KO → WT mice were subjected to DSS induced colitis.

Histological analysis

Colon tissues were fixed in 4% paraformaldehyde and embedded in paraffin. Dewaxed and rehydrated sections (5 μm) were subjected to H&E staining to assess the colon injury and the inflammatory status. Pathogenic scores of inflamed colons were evaluated by combining disease activity index (DAI) score and histopathological score by two researchers blindly. DAI core was assessed for each animal as a cumulative score for severity of colitis, according to weight loss (score: 0, none; 1, 1–5%; 2, 6–10%; 3, 11–18%; 4, >18%), stool consistency (score: 0, normal; 1,soft but still formed; 2, soft and loose stools; 3, very soft and wet; 4, watery diarrhea) and blood (score: 0, normal; 1 and 2, focal bloody stool; 3, blood traces in stool; 4, gross rectal bleeding). Histopathological changes were analyzed as a cumulative score, on the basis of epithelial damage (0, normal morphology; 1, loss of goblet cells; 2, loss of goblet cells in large areas; 3, loss of crypts; 4, loss of crypts in large areas) and inflammatory cell infiltration (0, no infiltration; 1, infiltration

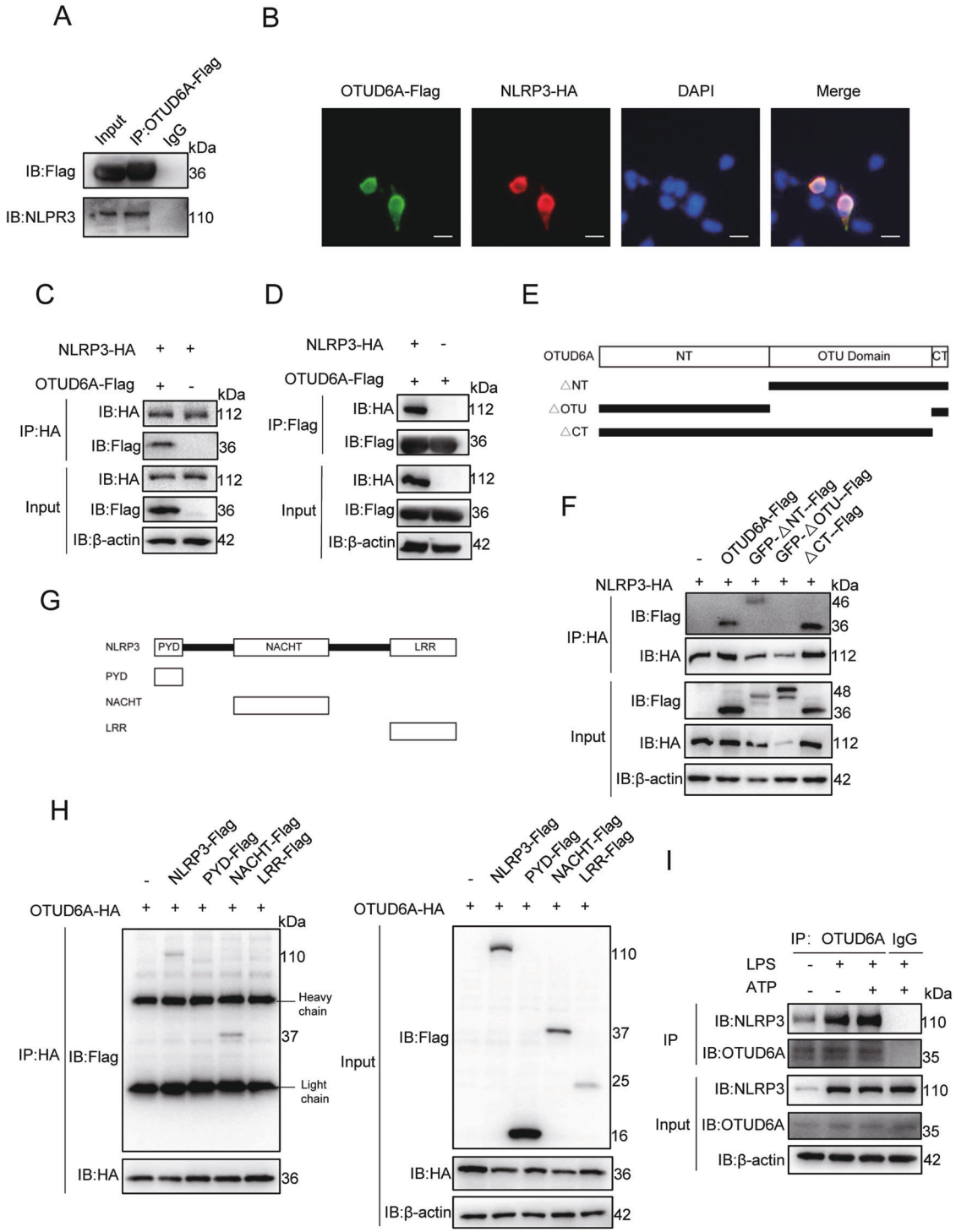

Fig. 6 OTUD6A directly interacts with NLRP3. A Co-IP assays showed that OTUD6A interacted with NLRP3 in HEK293T cells. Immunoprecipitations were performed using anti-FLAG magnetic beads. **B** Colocalization between OTUD6A and NLRP3 was examined by fluorescence microscopy in HEK293T cells. Immunoprecipitation analysis of the interaction of OTUD6A with NLRP3 by anti-HA magnetic beads (**C**) or anti-Flag magnetic beads (**D**), using NLRP3-HA and OTUD6A-Flag co-transfected into HEK293T cells. **E** Schematic diagram of OTUD6A and its truncated mutants. **F** Flag-tagged OTUD6A or its truncated mutants transfected into HEK293T cells with HA-tagged NLRP3. The cell lysates were immunoprecipitated with anti-HA magnetic beads and then immunoblotted with the indicated antibodies. **G** Schematic diagram of NLRP3 and its truncated mutants. **H** Flag-tagged NLRP3 or its truncated mutants transfected into HEK293T cells with HA-tagged OTUD6A. The cell lysates were immunoprecipitated with anti-HA magnetic beads and then immunoblotted with the indicated antibodies. **I** IP analysis of endogenous interaction of OTUD6A and NLRP3 in LPS-stimulated or LPS-primed and ATP-activated BMDMs. For all immunoblot data, similar results were obtained from three independent experiments.

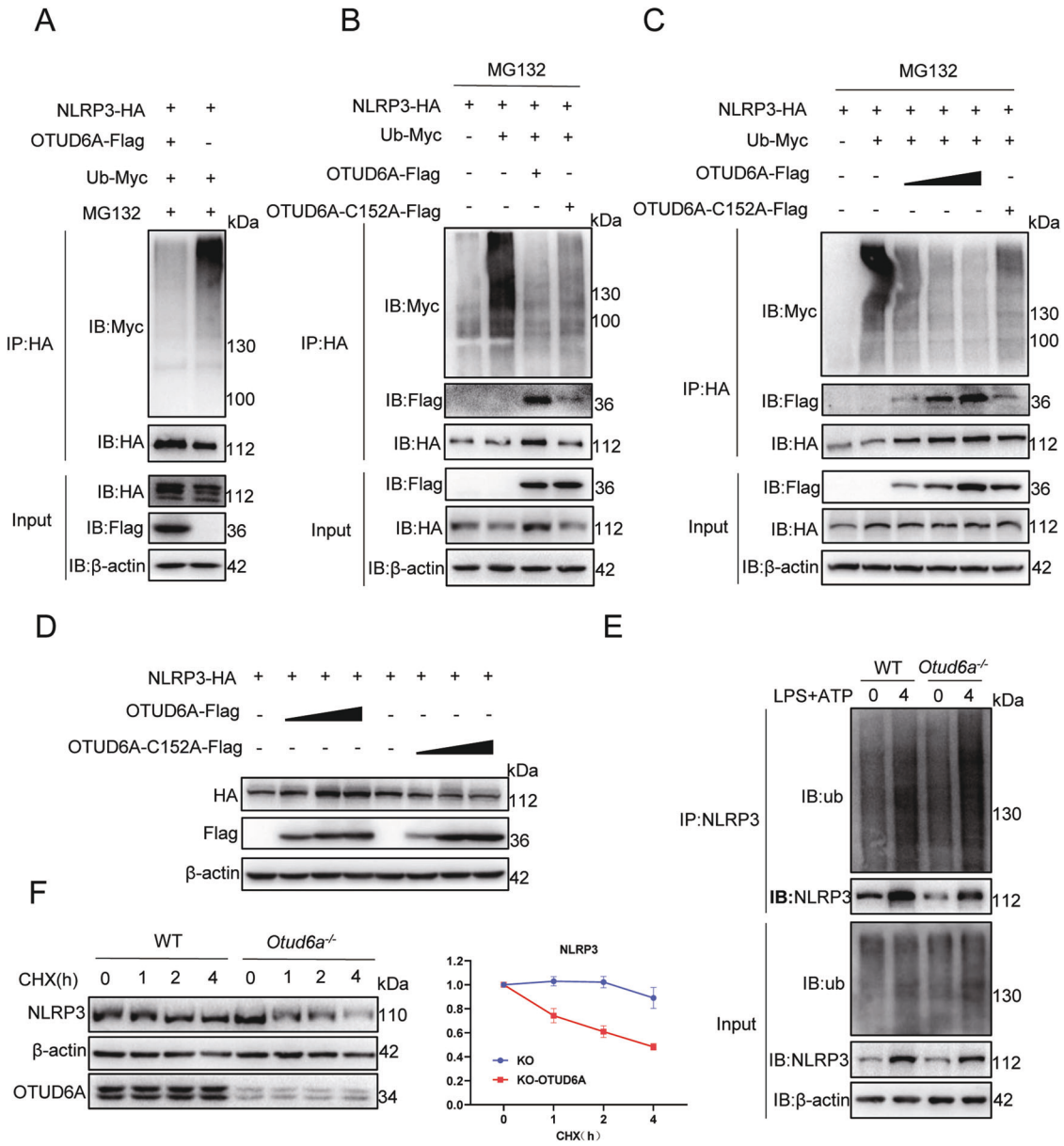

Fig. 7 OTUD6A deubiquitinates NLRP3. A Immunoblot analysis of the ubiquitination of NLRP3 in HEK293T cells co-transfected with Ub-Myc, NLRP3-HA and OTUD6A-Flag, followed by IP with anti-HA magnetic beads. Cells were pretreated with 10 μM of MG132 for 6 h before harvesting. **B** Immunoblot analysis of the ubiquitination of NLRP3 in HEK293T cells co-transfected with Ub-Myc, NLRP3-HA together with OTUD6A-Flag or OTUD6A-C152A-Flag, followed by IP with anti-HA magnetic beads. Cells were pretreated with 10 μM of MG132 for 6 h before harvesting. **C** Immunoblot analysis of the ubiquitination of NLRP3 in HEK293T cells co-transfected with Ub-Myc, NLRP3-HA, and increasing concentrations of vectors for the OTUD6A-Flag. Cells were pretreated with 10 μM of MG132 for 6 h before harvesting. **D** Immunoblot analysis of lysates from HEK293T cells co-transfected with NLRP3-HA, and increasing concentrations of vectors for the OTUD6A-Flag, or OTUD6A-C152A-Flag. **E** WT or *Otud6a*$^{-/-}$ BMDMs were treated with LPS + ATP at the indicated time point. The cell lysates were subjected to immunoprecipitation with anti-NLRP3 antibody and immunoblotting with anti-ubiquitin, NLRP3 and β-actin antibodies. **F** WT or *Otud6a*$^{-/-}$ BMDMs were treated with cycloheximide (100 μg/mL) at the indicated time points. Cell lysates were then collected for immunoblotting and representative image was shown (left panel). Quantification of the protein levels of NLRP3 (right panel). For all immunoblot data, similar results were obtained from three independent experiments. Statistical data are presented as mean ± SD.

around crypt bases; 2, infiltration spreading to muscularis mucosa; 3, extensive infiltration in the muscularis mucosa with abundant edema; 4, infiltration spreading to submucosa) as previously described [43].

Immunohistochemistry

Dewaxed and rehydrated sections were subjected to antigen retrieval in boiling water bath in 0.01 M citrate buffer (pH 6.0) for 2 min, then endogenous peroxidases were blocked with 0.3% hydrogen peroxidase for 10 min, followed by incubation in 5% normal goat serum (Solarbio, Beijing, China) for 30 min to prevent nonspecific antigen binding. The sections were then incubated with the primary antibodies against F4/80 (1:400), LYG6 (1:100) and Ki67 (1:200) for 2 h at room temperature. HRP-linked secondary antibodies and DAB were used for color development. Next, the sections were dehydrated using an alcohol gradient and sealed with neutral gum. All images were taken using bright-field illumination on an epifluorescence microscope equipped with digital camera (Nikon, Tokyo, Japan). The percentages of colonic samples that stained positive for OTUD6A were analyzed independently by two researchers blindly. Goblet cells were assessed by Periodic acid-Schiff/Alcian blue staining (PAS/AB) (Solarbio, Beijing, China). TUNEL staining was conducted using a kit from Beyotime

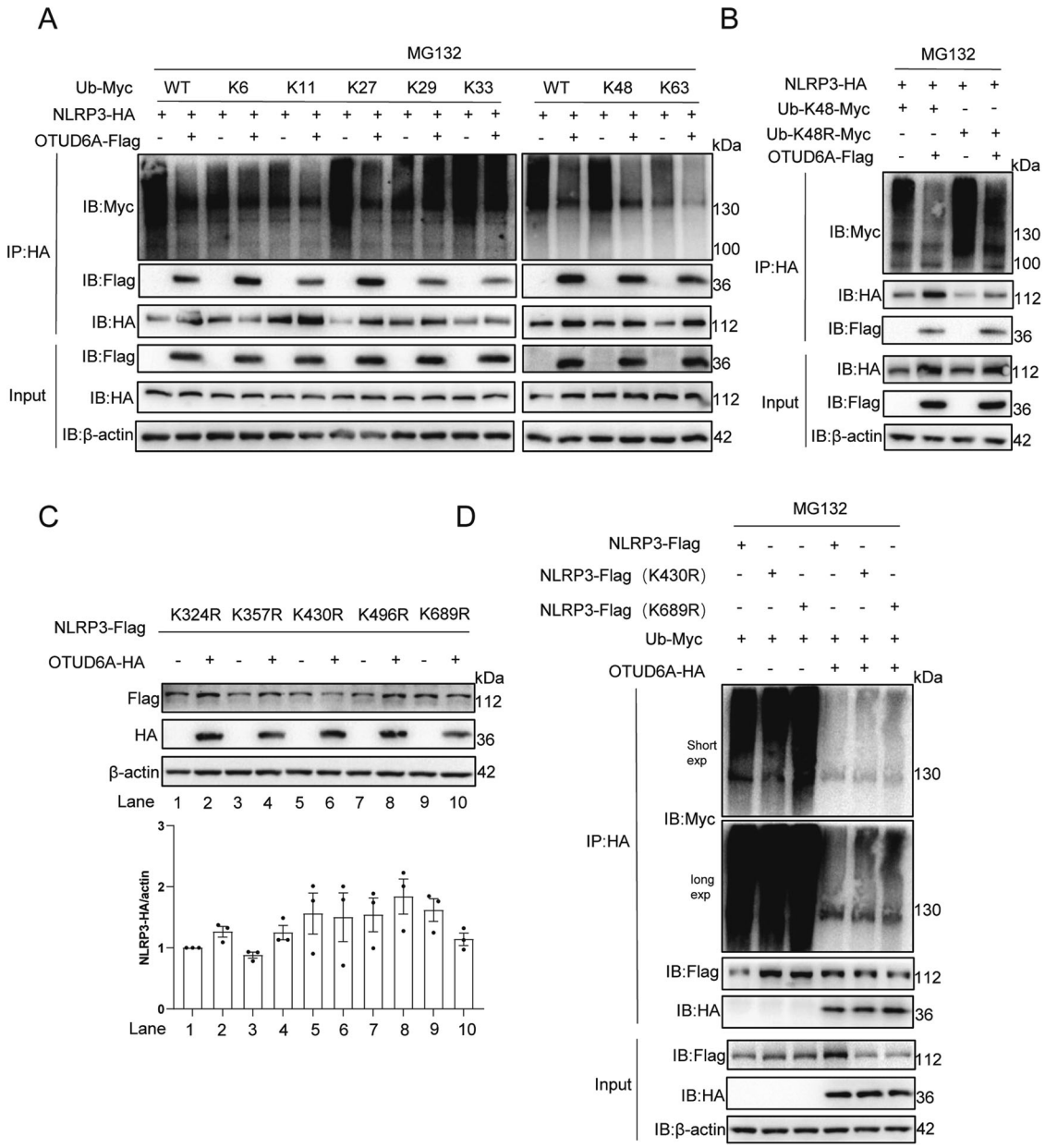

Fig. 8 OTUD6A stabilizes NLRP3 by cleaving its polyubiquitin chain at K430 and K689. A Immunoblot analysis of the ubiquitination of NLRP3 in HEK293T cells co-transfected with NLRP3-HA, OTUD6A-Flag, and various types of Ub-Myc including WT, K6-, K11-, K27-, K29-, K33-, K48-, and K63-linked ubiquitin chains for 24 h and then followed by IP with anti-HA magnetic beads. Cells were pretreated with 10 μM of MG132 for 6 h before harvesting. **B** Immunoblot analysis of the ubiquitination of NLRP3 in HEK293T cells co-transfected with NLRP3-HA, OTUD6A-Flag, Ub-K48-Myc or Ub-K48R-Myc, followed by IP with anti-HA magnetic beads. Cells were pretreated with 10 μM of MG132 for 6 h before harvesting. **C** Immunoblot analysis of lysates from HEK293T cells co-transfected with OTUD6A-HA and NLRP3-Flag WT or its mutants, and the lysates were analyzed by immunoblot analysis and representative images were shown (upper panel). Quantification of the protein levels of Flag-NLRP3 and its mutants (lower panel). **D** Immunoprecipitation and immunoblot analysis of HEK293T cells co-transfected with OTUD6A-HA, Ub-Myc and NLRP3-Flag WT, or the indicated mutants. For all immunoblot data, similar results were obtained from three independent experiments.

(C1086). ImageJ analysis software version 1.38e (National Institutes of Health, Bethesda, MD) was used for quantification of positive aera of PAS/AB staining, Ki67 staining, F4/80 staining, LY6G staining and TUNEL staining.

Immunofluorescence microscopy

Frozen sections and HEK293T cells transiently transfected with specific plasmids were fixed in 4% paraformaldehyde for 15 min, then labeled with primary antibodies overnight, followed by incubation of suitable fluorophore-conjugated secondary antibodies for 1 h at 37 °C. The primary antibodies were as follows: F4/80 (Cat#: 30325 S, 1:400, CST), HA-tag (Cat#: 51064-2-AP, 1:100, Proteintech), Flag-tag (Cat#: 66008-4-Ig, 1:1000, Proteintech). Nuclei were visualized through DAPI staining. Immunofluorescence images were obtained using a fluorescence microscope with DP2-BSW software (version 2.2, Olympus).

Enzyme-linked immunosorbent assay

Protein levels of TNF-α in colon tissues supernatant and IL-1β in serum and colon tissues supernatant were determined using TNF-α ELISA Kit (Cat#: 88-7324-76, ThermoFisher, Carlsbad, CA) and IL-1β Mouse ELISA Kit (Cat#: 88-7013-77, ThermoFisher, Carlsbad, CA) according to the manufacturer's protocol. The colon tissues supernatant was collected from tissue homogenized in lysis of mice treated with 2.5% DSS or AOM/DSS.

Lactate dehydrogenase assay

The release of LDH into the culture medium was determined using Lactate dehydrogenase assay kit (Cat#: A020-2-2, Nanjing Jiancheng, Nanjing, China) according to the manufacturer's instructions.

ASC speck staining

BMDMs were seeded at 5×10^5/ml in the glass bottom of 6-well plates. Cells were primed with 100 ng/ml LPS for 4 h and treated with 10 μM nigericin for 45 min. After that, cells were washed in PBS, and fixed with 4% paraformaldehyde, and permeabilized with 0.5% Triton X-100 for 10 min at room temperature. Cells were blocked with 5% bovine serum albumin for 1 hour at room temperature and then with anti-ASC antibody (1:200 dilution) overnight at 4 °C, followed by incubation of suitable fluorophore-conjugated secondary antibodies for 1 h at room temperature. After washing three times, nuclei were stained with DAPI. Cells were visualized and analyzed by TI-S fluorescence microscope (Nikon, Tokyo, Japan).

In vivo LPS challenge

WT and *Otud6a*$^{-/-}$ mice were injected intraperitoneally with LPS (20 mg/kg body weight). After 4 h, they were sacrificed and the serum concentrations of IL-1β and TNF-α were measured by ELISA (ThermoFisher).

Co-immunoprecipitation

The transfected cells were lysed with NP-40 Lysis Buffer (50 mM Tris-HCl pH 7.4, 150 mM NaCl, 1% NP-40) supplemented with protease inhibitor cocktail (Cat#: P1045, Beyotime) on ice before sonicating for 1 min then centrifugation at $12{,}000 \times g$ at 4 °C for 15 min. 1/10 volume of the supernatant is retained as input, the remaining was incubated with anti-HA Magnetic beads or anti-Flag Magnetic beads overnight on a rotator at 4 °C. The immunocomplexes were then washed with 500 μL of lysis buffer 5 times and eluted with SDS buffer.

Western blot analysis

Colon tissues and cells were homogenized in RIPA buffer (Cat#: P0013B, Beyotime) containing protease and phosphatase inhibitor cocktail (Cat#: P1051, Beyotime). Protein concentrations were measured using a quick start bradford kit (Bio-Rad, Hercules, CA). Approximately 35 μg protein was loaded and electrophoresed in SDS–polyacrylamide gels electrophoresis and transferred to polyvinylidene difluoride membrane (Bio-Rad). Membranes were then blocked with 5% skim milk for 1 h, and then incubated overnight with primary antibodies. After incubated with HRP-linked secondary antibodies, specific protein bands were visualized with a ChemiDoc XRS + system (Bio-Rad). Image J analysis software version 1.38e (NIH, Bethesda, MD) was used for densitometric quantification of blots.

RNA-Seq and Data Processing

BMDMs from WT and *Otud6a*$^{-/-}$ mice were plated at 3×10^5 cells/well in six-well plates. Cells were challenged with PBS or 100 ng/mL LPS for 6 h. Cells were then collected in TRIzol reagent. Three biological replicates were performed for each group. RNA-seq analysis was performed at Hangzhou Lc-Bio Technologies Co.,Ltd, China. The original RNA sequencing data are uploaded in the open-access Gene Expression Omnibus (GSE224239, https://www.ncbi.nlm.nih.gov/geo/).

RNA extraction and quantitative real-time PCR

Mouse colon tissues and BMDMs cells were lyzed in TRIzol (Invivogen) for total RNA extraction. cDNAs were synthetized using TransScript® All-in-One First-Strand cDNA Synthesis SuperMix for qPCR (TransGen Biotech, Beijing, China). RT-qPCR were performed using PerfectStart® Green qPCR SuperMix (transgen biotech, Beijing, China) on CFX96 Touch Real-Time PCR Detection System (Bio-Rad). Primer sequences are listed in Supplementary Table S2.

Statistical Analyses

All results are presented as mean ± SD. Statistical analyses were performed using GraphPad Prism 8. Kolmogorov–Smirnov test was used to validate the normal distribution of all data. Student's *t*-test was used to compare two groups of data. One-way ANOVA followed by Dunnett's post-hoc test was used to compare more than two groups of data. For the mouse survival study, Kaplan-Meier survival curves were generated, and a log-rank test was used to determine statistical significance. All the statistical data were presented as mean ± SD. $P < 0.05$ was considered significant. Post-tests were performed if the F achieved was at $p < 0.05$, and there was no significant variance inhomogeneity. The statistical tests were justified as appropriate according to assessment of normality and variance of the distribution of the data. No randomization or exclusion of data points was used. No 'blinding' of investigators was applied.

DATA AVAILABILITY

All data needed to evaluate the conclusions in this study are presented in this manuscript or the supplementary information. The materials described in this study are either commercially available or available upon reasonable request from the corresponding authors.

REFERENCES

1. Na YR, Stakenborg M, Seok SH, Matteoli G. Macrophages in intestinal inflammation and resolution: a potential therapeutic target in IBD. Nat Rev Gastroenterol Hepatol. 2019;16:531–43.
2. Wallace KL, Zheng LB, Kanazawa Y, Shih DQ. Immunopathology of inflammatory bowel disease. World J Gastroenterol. 2014;20:6–21.
3. Roda G, Ng SC, Kotze PG, Argollo M, Panaccione R, Spinelli A, et al. Crohn's disease. Nat Rev Dis Primers 2020;6:22.
4. Kobayashi T, Siegmund B, Le Berre C, Wei SC, Ferrante M, Shen B, et al. Ulcerative colitis. Nat Rev Dis Primers 2020;6:74.
5. Sung H, Ferlay J, Siegel RL, Laversanne M, Soerjomataram I, Jemal A, et al. Global cancer statistics 2020: GLOBOCAN estimates of incidence and mortality worldwide for 36 cancers in 185 countries. CA Cancer J Clin. 2021;71:209–49.
6. Siegel RL, Miller KD, Sauer AG, Fedewa SA, Butterly LF, Anderson JC, et al. Colorectal cancer statistics, 2020. CA Cancer J Clin. 2020;70:145–64.
7. Faye AS, Holmer AK, Axelrad JE. Cancer in inflammatory bowel disease. Gastroenterol Clin North Am. 2022;51:649–66.
8. Song Y, Yuan M, Xu Y, Xu H. Tackling inflammatory bowel diseases: targeting proinflammatory cytokines and lymphocyte homing. Pharmaceuticals 2022;15:1080.
9. Ruan J, Schluter D, Naumann M, Waisman A, Wang X. Ubiquitin-modifying enzymes as regulators of colitis. Trends Mol Med. 2022;28:304–18.
10. Popovic D, Vucic D, Dikic I. Ubiquitination in disease pathogenesis and treatment. Nat Med. 2014;20:1242–53.
11. Clague MJ, Barsukov I, Coulson JM, Liu H, Rigden DJ, Urbe S. Deubiquitylases from genes to organism. Physiol Rev. 2013;93:1289–315.
12. Bednash JS, Mallampalli RK. Regulation of inflammasomes by ubiquitination. Cell Mol Immunol. 2016;13:722–8.
13. Lei H, Yang L, Xu HZ, Wang ZT, Li XY, Liu M, et al. Ubiquitin-specific protease 47 regulates intestinal inflammation through deubiquitination of TRAF6 in epithelial cells. Sci China-Life Sci. 2022;65:1624–35.
14. Wu B, Qiang LH, Zhang Y, Fu YS, Zhao MY, Lei ZH, et al. The deubiquitinase OTUD1 inhibits colonic inflammation by suppressing RIPK1-mediated NE-kappa B signaling. Cell Mol Immunol. 2022;19:276–89.
15. Shi L, Liu J, Peng YH, Zhang JF, Dai XP, Zhang SX, et al. Deubiquitinase OTUD6A promotes proliferation of cancer cells via regulating Drp1 stability and mitochondrial fission. Mol Oncol. 2020;14:3169–83.
16. Peng YH, Liu J, Wang Z, Cui CP, Zhang TT, Zhang SX, et al. Prostate-specific oncogene OTUD6A promotes prostatic tumorigenesis via deubiquitinating and stabilizing c-Myc. Cell Death Differ. 2022;29:1730–43.
17. Zhao Y, Huang XP, Zhu D, Wei M, Luo JC, Yu SY, et al. Deubiquitinase OTUD6A promotes breast cancer progression by increasing TopBP1 stability and rendering tumor cells resistant to DNA-damaging therapy. Cell Death Differ. 2022;29:2531–44.
18. Yao D, Dong M, Dai C, Wu S. Inflammation and inflammatory cytokine contribute to the initiation and development of ulcerative colitis and its associated cancer. Inflamm Bowel Dis. 2019;25:1595–602.
19. Zhen Y, Zhang H. NLRP3 Inflammasome and inflammatory bowel disease. Front Immunol. 2019;10:276.
20. Zhou LL, Liu T, Huang B, Luo M, Chen ZH, Zhao ZY, et al. Excessive deubiquitination of NLRP3-R779C variant contributes to very-early-onset inflammatory bowel disease development. J Allergy Clin Immunol. 2021;147:267–79.
21. Py BF, Kim MS, Vakifahmetoglu-Norberg H, Yuan JY. Deubiquitination of NLRP3 by BRCC3 Critically Regulates Inflammasome Activity. Mol Cell. 2013;49:331–8.
22. Ren GM, Zhang XY, Xiao Y, Zhang W, Wang Y, Ma WB, et al. ABRO1 promotes NLRP3 inflammasome activation through regulation of NLRP3 deubiquitination. Embo J. 2019;38:e100376.
23. Palazon-Riquelme P, Worboys JD, Green J, Valera A, Martin-Sanchez F, Pellegrini C, et al. USP7 and USP47 deubiquitinases regulate NLRP3 inflammasome activation. Embo Rep. 2018;19:e44766.

24. Liu T, Wang LQ, Liang PP, Wang XJ, Liu YK, Cai J, et al. USP19 suppresses inflammation and promotes M2-like macrophage polarization by manipulating NLRP3 function via autophagy. Cell Mol Immunol. 2021;18:2431–42.
25. Wang D, Zhang YN, Xu XM, Wu JF, Peng Y, Li J, et al. YAP promotes the activation of NLRP3 inflammasome via blocking K27-linked polyubiquitination of NLRP3. Nat Commun. 2021;12:2674.
26. Song H, Liu BY, Huai WW, Yu ZX, Wang WW, Zhao J, et al. The E3 ubiquitin ligase TRIM31 attenuates NLRP3 inflammasome activation by promoting proteasomal degradation of NLRP3. Nat Commun. 2016;7:13727.
27. Yan CY, Ouyang SH, Wang X, Wu YP, Sun WY, Duan WJ, et al. Celastrol ameliorates Propionibacterium acnes/LPS-induced liver damage and MSU-induced gouty arthritis via inhibiting K63 deubiquitination of NLRP3. Phytomedicine. 2021; 80:153398.
28. Pu T, Liu WZ, Wu YJ, Zhao Y. A20 functions as a negative regulator in macrophage for DSS-induced colitis. Int Immunopharmacol. 2021;97:107804.
29. Zhou MX, He J, Shi YY, Liu XM, Luo SJ, Cheng C, et al. ABIN3 negatively regulates necroptosis-induced intestinal inflammation through recruiting A20 and restricting the ubiquitination of RIPK3 in inflammatory bowel disease. J Crohns Colitis. 2021;15:99–114.
30. Leszczynska K, Jakubczyk D, Gorska S. The NLRP3 inflammasome as a new target in respiratory disorders treatment. Front Immunol. 2022;13:1006654.
31. Zheng Y, Xu L, Dong N, Li F. NLRP3 inflammasome: The rising star in cardiovascular diseases. Front Cardiovasc Med. 2022;9:927061.
32. Khot M, Sood A, Tryphena KP, Khan S, Srivastava S, Singh SB, et al. NLRP3 inflammasomes: a potential target to improve mitochondrial biogenesis in Parkinson's disease. Eur J Pharmacol. 2022;934:175300.
33. Cui S, Wang CH, Bai WZ, Li J, Pan Y, Huang XY, et al. CD1d1 intrinsic signaling in macrophages controls NLRP3 inflammasome expression during inflammation. Sci Adv. 2020;6:eaaz7290.
34. Song Y, Zhao Y, Ma Y, Wang Z, Rong L, Wang B, et al. Biological functions of NLRP3 inflammasome: A therapeutic target in inflammatory bowel disease. Cytokine Growth factor Rev. 2021;60:61–75.
35. Bauer C, Duewell P, Mayer C, Lehr HA, Fitzgerald KA, Dauer M, et al. Colitis induced in mice with dextran sulfate sodium (DSS) is mediated by the NLRP3 inflammasome. Gut. 2010;59:1192–9.
36. Li H, Guan Y, Liang B, Ding P, Hou X, Wei W, et al. Therapeutic potential of MCC950, a specific inhibitor of NLRP3 inflammasome. Eur J Pharmacol. 2022;928:175091.
37. Juliana C, Fernandes-Alnemri T, Kang S, Farias A, Qin F, Alnemri ES. Non-transcriptional priming and deubiquitination regulate NLRP3 inflammasome activation. J Biol Chem. 2012;287:36617–22.
38. Yu P, Zhang X, Liu N, Tang L, Peng C, Chen X. Pyroptosis: mechanisms and diseases. Signal Transduct Target Ther. 2021;6:128.
39. Xu T, Yu WW, Fang H, Wang Z, Chi ZX, Guo XC, et al. Ubiquitination of NLRP3 by gp78/Insig-1 restrains NLRP3 inflammasome activation. Cell Death Differ. 2022;29:1582–95.
40. Song H, Zhao CY, Yu ZX, Li QZ, Yan RZ, Qin Y, et al. UAF1 deubiquitinase complexes facilitate NLRP3 inflammasome activation by promoting NLRP3 expression. Nat Commun. 2020;11:6042.
41. Tang J, Tu S, Lin GX, Guo H, Yan CK, Liu QJ, et al. Sequential ubiquitination of NLRP3 by RNF125 and Cbl-b limits inflammasome activation and endotoxemia. J Exp Med. 2020;217:e20182091.
42. Liu X, Luo W, Chen J, Hu C, Mutsinze RN, Wang X, et al. USP25 deficiency exacerbates acute pancreatitis via up-regulating TBK1-NF-kappaB signaling in macrophages. Cell Mol Gastroenterol Hepatol. 2022;14:1103–22.
43. Wirtz S, Neufert C, Weigmann B, Neurath MF. Chemically induced mouse models of intestinal inflammation. Nat Protoc. 2007;2:541–6.

ACKNOWLEDGEMENTS

We graciously thank Fuping You (Peking University, Beijing, China) for sharing *Otud6a*$^{-/-}$ mice. This study was supported by the National Natural Science Foundation of China (81970338 and 82170373 to YW), Medical and Health Research Project of Zhejiang Province (2023XY164 to LH), and Key Scientific Project of Wenzhou City (ZY2021021 to YW).

AUTHOR CONTRIBUTIONS

XLiu, GL and YW contributed to the literature search and study design. XLiu, YF, XLv, CH, LZ and BJ performed the experiments and analyzed the data. GC, LH and WL provided technical help. XLiu, GL and YW participated in the drafting of the article. All authors agree to be accountable for all aspects of work ensuring integrity and accuracy.

COMPETING INTERESTS

The authors declare no competing interests.

ETHICS APPROVAL

The study about the human colonic biopsy samples was approved by the Human Ethical Committee of the Quzhou People's Hospital (Approval document #2022–0037). All animal studies were approved by the Institutional Animal Policy and Welfare Committee of Wenzhou Medical University (Approval document #wydw2022-0202).

ADDITIONAL INFORMATION

Supplementary information The online version contains supplementary material available at https://doi.org/10.1038/s41418-023-01148-7.

Correspondence and requests for materials should be addressed to Yi Wang.

Reprints and permission information is available at http://www.nature.com/reprints

Publisher's note Springer Nature remains neutral with regard to jurisdictional claims in published maps and institutional affiliations.